Available online at www.sciencedirect.com
SCIENCE DIRECT®
Materials Chemistry and Physics 87 (2004) 411–419
MATERIALS CHEMISTRY AND PHYSICS
www.elsevier.com/locate/matchemphys

Effect of α-Al_2O_3 particles on the electrochemical codeposition of Co–Ni alloys from sulfamate electrolytes

Gang Wu [a,*], Ning Li [b], Dian Long Wang [b], De Rui Zhou [b], Bo Qing Xu [a], Kurachi Mitsuo [c]

[a] *Innovative Catalysis Program, Key Laboratory of Organic Optoelectronics & Molecular Engineering, Department of Chemistry, Tsinghua University, Beijing 100084, PR China*
[b] *Department of Applied Chemistry, Harbin Institute of Technology, Harbin 150001, PR China*
[c] *Faculty of Engineering, Kyoto University, Kyoto 606-8283, Japan*

Received 14 March 2004; received in revised form 7 June 2004; accepted 11 June 2004

Abstract

The effect of α-Al_2O_3 particles on the electrochemical codeposition behaviour of Co–Ni alloys from sulfamate electrolyte was investigated by codeposition experiments, zeta potential and electrochemical methods. The results indicate that the presence of Al_2O_3 particles in Co–Ni sulfamate electrolytes contributes to the preferential codeposition of Co. Moreover, increasing Co^{2+} concentration also can enhance the codeposition of Al_2O_3 particles in Co–Ni alloy matrix. Zeta potential measurements confirm that Co^{2+} has a stronger tendency to adsorb on Al_2O_3 particles surface than Ni^{2+} does in sulfamate electrolytes. Steady-state polarization and electrochemical impedance spectroscopy (EIS) show that the effect of Al_2O_3 particles on electrochemical codeposition behaviour of Co–Ni alloy in different Co^{2+}/Ni^{2+} ratio electrolytes (1:5 and 5:1) is quite contrary. In nickel-rich electrolytes ($Co^{2+}/Ni^{2+} = 1:5$), the Al_2O_3 particles cause a negative shift in reduction potential and an increase of charge transfer resistance. However, in cobalt-rich electrolytes ($Co^{2+}/Ni^{2+} = 5:1$), Al_2O_3 particles lead to a positive shift of reduction potential and reduce the charge transfer resistance. Moreover, in EIS, besides one capacitive loop at high frequency and one inductive loop at low frequency, the introduction of Al_2O_3 particles leads to a further inductive loop at low frequency. According to simulated results of EIS, an electrochemical codeposition mechanism of Al_2O_3 particles with Co–Ni alloys is presented and in good agreement with the experimental results.

Keywords: Electrochemical codeposition; Composite codeposition; Zeta potential; Alumina; Co–Ni alloys

1. Introduction

Recently, interest in electrodeposited composite coatings has increased rapidly due to their attractive properties derived from the combination of particles dispersed in the matrix [1–3]. Besides the large-scale application of composite coatings as wear resistant layers, such as Ni–SiC [4–7], Ni–Al_2O_3 [8], Ni–ZrO_2 [9] and Co–TiO_2 [10] there is interest in new type composite coatings with unique physical and chemical properties. Examples are the improvement of adhesion of paint top layers onto zinc coatings through the incorporation of silica particles [11], and the synthesis of catalytic coatings like Ni–FeS_x [12], Ni–MoS_2 [13], Ni–RuO_2 [14,15] and Ni–Co–$LaNi_5$ [16] having low overpotential for hydrogen evolution reaction.

In general, the codeposition of solid particles with metals to obtain composite coatings involves two adsorption processes. Firstly, cations such as hydrogen ions and metal ions are adsorbed on the particle surfaces; secondly, solid particles, after reaching the cathode, undertake adsorption [17,18].

As for the adsorption of cations on particle surface, many investigations were carried out for various electrolytes and particles. The adsorption of cations on the solid particles not only affects the surface charge but also determines the codeposition process. In earlier years, Fink and Prince [19] realized the importance of surface charge and stated that a positive surface charge can enhance codeposition, because the particles are electrostatically attracted to the cathode. This was confirmed by Tomaszewski et al. [20], who found that the negatively charged silica particles transported less readily to the cathode than positively charged Al_2O_3 particles. Furthermore, Tomaszewski had suggested that particles can be obtained positive charge by adsorption of metal

* Corresponding author. Tel.: +86-10-62795834; fax: +86-10-62792122.
E-mail address: wugang1976@hotmail.com (G. Wu).

0254-0584/$ – see front matter © 2004 Elsevier B.V. All rights reserved.
doi:10.1016/j.matchemphys.2004.06.016

ions or H^+ ions. Kariapper and Foster [21] noticed that the amount of adsorbed metal ions increased with increasing metal ion concentration or the addition of some promoter such as Tl^+. Meguno et al. [22] confirmed the zeta potentials as a quantitative measurement for the particle surface charge. At high pH, the zeta potential of SiC is negative, but it increases with decreasing pH and becomes positive at low pH. Lee and Wan [23] investigated the zeta potential of Al_2O_3 particles in a dilute copper sulfate bath. First, the zeta potential of α-Al_2O_3 increases with copper sulfate concentration and becomes positive, while γ-Al_2O_3 becomes more negative. The results explained why α-Al_2O_3 could be codeposited much more easily than γ-Al_2O_3 with copper. Second, codeposition promoters like Tl^+ cause a large increase in zeta potential to positive values.

Adsorption of particles on the electrode surface is a very important and intensively studied phenomenon, which became the basis for the technology of electrochemical composite codeposition. Besides the particle surface charge, there are many other factors affecting the interaction between particles and electrode surface including particle concentration, particle structure, bath composition, current density, temperature, pH, agitation and the presence of surfactants. It is difficult to build a precise model to elucidate the interaction between particles and electrode surface, which takes into account all parameters. A first mathematic description of the electrochemical codeposition by Guglielmi was based on a two-step codeposition mechanism [24]. Guglielmi assumed that particles are first reversibly adsorbed on the electrode surface. These loosely adsorbed particles are then embedded in an electrochemical step. Considering the reduction of the metal ions adsorbed on the particle surfaces as the key step in codeposition, Celis et al. [25] derived an equation, which allows a prediction of codeposition for systems of defined hydrodynamics. An attempt to develop a predictive model was undertaken by Fransaer et al. [26]. The number of particles reaching the surface of a rotating disc electrode was calculated using a trajectory analysis with all forces acting on a particle. Based on hypotheses concerning the effective adsorption and the distribution of the adsorption strength of particles on the cathode, Wang et al. [27] developed an adsorption strength model and described the mechanism of codeposition of Al_2O_3 with Fe–P alloy. Only when the adsorption strength between particles and cathode surface is above a critical value, is the adsorption of these particles effective and can be incorporated into the deposit.

To investigate the two kind interactions during composite electrodeposition from the standpoint of electrochemistry, polarization curves and electrochemical impedance spectroscopy (EIS) are powerful tools for determining these interactions [4,28]. It was found from Socha et al. [29] that when SiC particles codeposited with nickel, the current density decreased and simultaneously the Faradaic reaction resistance of the electrode process increased. However, when silica particles were added to the plating bath, current density increased and the Faradaic reaction resistance decreased, despite the fact that no codeposition of SiO_2 particles was observed. Increased current in the polarization behaviour at a fixed potential was attributed to the increased surface area due to the adsorption of particles. Watson [30] compared the codeposition of conductive particles, Cr, and semi-conductive particles, SiC, with nickel on a vitreous carbon surface. They reported that the SiC particles in sulfate electrolyte showed a 130 mV positive displacement of nickel reduction, while Cr particles exhibited a 110 mV positive displacement. They suggested that the effect of SiC particles on nickel electrodeposition was to catalyze the reduction of H^+ and Ni^+_{ads} intermediates. Yeh and Wan [4] studied the codeposition of SiC particles with nickel by EIS and indicated that SiC particles not only increase the adsorption of Ni^+_{ads} intermediate near the electrode but also produce a shielding effect on the active surface during electrodeposition. Benea and Carac [31] also reported that SiC particles on the electrode surface cause a strong influence on impedance during nickel electrodeposition.

At present work, taking into account the exceptional advantages of Co–Ni alloy such as mechanical properties [32], chemical and physical properties (electrocatalytic activity [33,34], magnetism [35]), composite coatings based on Co–Ni alloy matrix can be used in many industrial fields. The electrodeposition of Co–Ni alloys, whether from single or complex electrolytes, belongs to the anomalous type, in which less noble metal (cobalt) is preferentially deposited. Earlier work has been directed toward understanding of the alloy codeposition phenomenon in different electrolytes [36–40]. However, despite having both practical and theoretical importance, the effects of inert particles on the anomalous codeposition of Co–Ni alloy are not well understood and related literatures are scanty. The aim of this work is to investigate the interactions between α-Al_2O_3 particles and metal ions as well between particles and electrode surfaces and to determine the effects of α-Al_2O_3 particles on the electrochemical behaviour of the Co–Ni alloy codeposition from sulfamate electrolytes.

2. Experimental details

2.1. Codeposition of α-Al_2O_3 with Co–Ni alloys

In order to investigate the codeposition of α-Al_2O_3 with Co–Ni alloys, the electrolytes containing different ratios of Co^{2+}/Ni^{2+} (1:5, 1:2, 1:1, 2:1, 5:1) were prepared by dissolving 50–250 g l^{-1} of $Co(NH_2SO_3)_2{\cdot}4H_2O$, 50–250 g l^{-1} of $Ni(NH_2SO_3)_2{\cdot}4H_2O$, 20 g l^{-1} of H_3BO_3 and 20 ml l^{-1} of CH_3NO in double distilled water, to which 20–140 g l^{-1} of α-Al_2O_3 particles was added. Reagents of analytical purity were used for preparing the solutions. Total metallic salt concentration ($Co(NH_2SO_3)_2{\cdot}4H_2O$ + $Ni(NH_2SO_3)_2{\cdot}4H_2O$) was kept constant 300 g l^{-1} and the concentrations of each metal ion in various ratio elec-

Table 1
Sulfamate electrolytes containing various Co^{2+}/Ni^{2+} ratios

No.	$Ni(SO_3NH_2)_2{\cdot}4H_2O$ ($g\,l^{-1}$)	$Co(SO_3NH_2)_2{\cdot}4H_2O$ ($g\,l^{-1}$)	Ni^{2+}/Co^{2+}
1	250	50	5:1
2	200	100	2:1
3	150	150	1:1
4	100	200	1:2
5	50	250	1:5

trolytes were shown in Table 1. Commercially available α-Al_2O_3 particles (HRA-5 Martinswerck) with specific gravity of 4.0 and over 99% purity were used in this study. The mean size of the α-Al_2O_3 particles was around 0.5 μm. The Al_2O_3 particles were pre-treated with acetone and 5% HNO_3 to remove residual organic and other impurities, then washed with distilled water and dried. In addition, an ultrasonic generator was used to minimize the agglomeration of Al_2O_3 particles in the suspension before codeposition.

The composite electrodeposition experiments were conducted in a 2 l capacity PVC container with heating facilities. Rectangular 80 mm × 40 mm copper plates were used as substrates for the cathodes. Separate rectangular 80 mm × 25 mm cobalt (99.0%) and nickel (99.9%) anodes were used. To maintain constant metal ion concentration in electrolytes, the dissolving rates of cobalt and nickel anodes were precisely controlled by adjusting the current density flowing though the different anodes. The electrolytes were operated at 50 and 60 °C, at a current density j_k of 3 A dm^{-2}. The pH was kept at 4.0 and the stirring rate was 100 rpm. In order to assess the influence of Al_2O_3 particles on codeposition, Co–Ni alloys were also electrodeposited under the same conditions without Al_2O_3 particles.

The volume fraction of Al_2O_3 particles in the composite coatings (denoted by V_p) was measured by gravimetric analysis. To determine the composition of the electrodeposited alloys, the deposits were stripped in an 1:3 HNO_3 solution, and then the amounts of cobalt and nickel were measured by atomic adsorption spectrum (AAS). The cathodic current efficiencies for composite codeposition were determined by a standard copper coulometer connected in series with the electrodeposition cell.

2.2. Zeta potential measurements

Electrokinetic properties of particles in solution play a key role in composite electrodeposition. They are generally evaluated according to their zeta potential, which determines the adsorption amount of H^+ and metal ions on the particle surfaces. Accordingly, measurements were done under different conditions using a MALVERN Zetasizer 3000HSA at 25 °C. To determine adsorption of H^+ ions on the α-Al_2O_3 particle surfaces, a specific amount of Al_2O_3 was added to the solutions, and the pH was adjusted with HNH_2SO_3 and NaOH at the same ionic concentration as sodium chloride (0.001 M). To keep the Al_2O_3 particles in a homogeneous suspension, a magnetic stirrer was used for 48 h before measurement. In order to investigate the adsorption of Co^{2+} and Ni^{2+} as well as the competitive adsorption between Co^{2+} and Ni^{2+}, solutions with different metal ion concentrations and different ratios of Co^{2+}/Ni^{2+} (1:5, 1:2, 1:1, 2:1, 5:1) were prepared at a constant pH of 4.0. The total metal ions concentration kept constant. Likewise, Al_2O_3 particles were added to these solutions stirred with a magnetic stirrer for 48 h. The solutions were then diluted 100 times to measure.

2.3. Electrochemical measurements

The electrochemical measurements were carried out in a conventional three-electrode cell at 25 °C. A large area Pt sheet was used as the counter electrode and a saturated calomel electrode (SCE) as the reference. Oxygen was removed from the solution by bubbling nitrogen gas (99.99%). The solution was stirred with a magnetically driven Teflon coated stirring bar. The steady state polarization curves for electrolytes with different particle and metal ion concentrations were measured using an EG&G PAR 273 Potentiostat–Galvanostat. The scan rate was 2 mV s^{-1}. All the steady-state overpotential values were corrected according to the electrolyte resistance value estimated from the electrochemical impedance spectroscopy (EIS). An EG&G PAR 1025 Frequency Response Detector was used for EIS measurements. The EIS were carried out between 10 kHz and 0.01 Hz frequency ranges (r.m.s. amplitude = 5 mV). Before starting data acquisition, the potential was applied to the electrode for 30 min. During the measurements nitrogen was passed over the electrolytes. All electrode potentials are referred to the standard hydrogen electrode (SHE).

3. Results

3.1. Codeposition of α-Al_2O_3 with Co–Ni alloys

Fig. 1 shows the relationship between Co contents in the deposit and Co^{2+} concentrations in solutions with and without Al_2O_3 particles. Whether Al_2O_3 particles were added or not, the percentage of Co in the deposit is always higher than that in solution. This indicates that the preferential anomalous codeposition behaviour of Co^{2+} was not changed by addition of Al_2O_3. Furthermore, the results indicate that

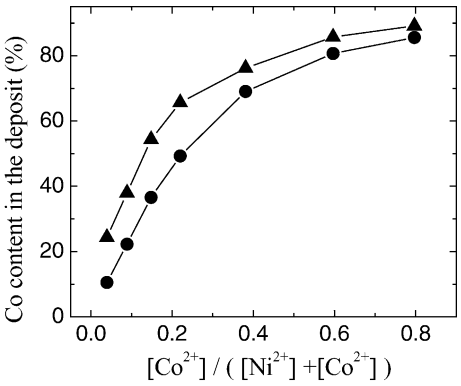

Fig. 1. Relationship of Co contents between solution and deposit from sulfamate electrolytes without (●) and with (▲) 80 g l^{-1} Al_2O_3 particles; pH = 4.0, j_k = 3 A dm^{-2}, T = 60 °C, 100 rpm.

Al_2O_3 particles lead to higher Co contents in the deposit and promote the codeposition of Co^{2+}.

As indicated in Fig. 2, keeping the ratio of $[Co^{2+}]/([Co^{2+}] + [Ni^{2+}])$ in the bath at 0.5 and constant total metal ion concentration, the volume fraction of Al_2O_3 in the deposit, V_p, increases with particle concentration, and then tends to attain a steady value at a concentration of 80 g l^{-1}. Furthermore, the V_p of Al_2O_3 at 50 °C is larger than that at 60 °C, although the higher temperature is helpful in reducing roughness and internal stress of the composite coatings.

Moreover, the curves are very similar to the well-known Langmuir adsorption isotherms, supporting a mechanism based on an adsorption effect. So the codeposition of Al_2O_3 may be attributed to the adsorption of Al_2O_3 particles on the cathode surface, as suggested by Guglielmi's two-step adsorption model [24]. Once the particle is adsorbed, the metal begins building around the particle slowly, encapsulating and incorporating it. The plateau observed at higher particle concentrations may be a result of saturation adsorption on the cathode surface.

The effect of Co^{2+} concentration on V_p is shown in Fig. 3. V_P increases with Co^{2+} concentration and holds up to 0.4 ratio of $[Co^{2+}]/([Co^{2+}] + [Ni^{2+}])$ with further marginal increment at higher Co^{2+} concentrations. Consequently, the codeposition of Al_2O_3 can be promoted by the adsorption of Co^{2+} on its surface, which increases the surface positive charge and enhances the adsorption strength between particles and cathode.

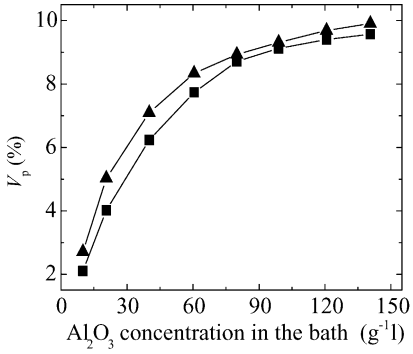

Fig. 2. Relationship between Al_2O_3 concentration in electrolytes and V_P from electrolytes containing 150 g l^{-1} cobalt sulfamate and 150 g l^{-1} nickel sulfamate. j_k = 3 A dm^{-2}, pH = 4.0, 100 rpm, T = 60 °C (■) and 50 °C (▲).

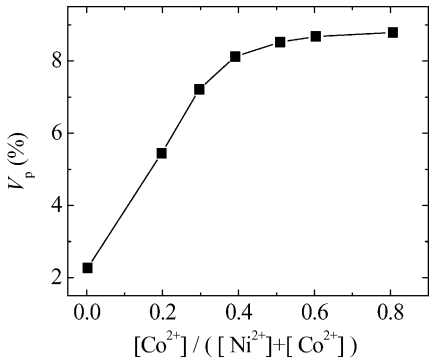

Fig. 3. The effect of Co^{2+} concentration in solutions on V_P; 80 g l^{-1} Al_2O_3, pH = 4.0, j_k = 3 A dm^{-2}, T = 60 °C, 100 rpm.

3.2. Zeta potential and current efficiency

In principle, a metal oxide particle like Al_2O_3 in an aqueous solution tends to polarize and to be electrically charged. This oxide is amphoteric; thus the nature and magnitude of this charge are a function of pH value. To determine the adsorption of H^+ on Al_2O_3 particle surfaces, the zeta potentials in solutions with different pH were measured and shown in Fig. 4. Clearly, the zeta potential increases with decreasing pH. This is due to the fact that more H^+ ions can adsorb on Al_2O_3 particle surface at lower pH levels. Fig. 4 also indicates that the zeta potential equals zero at pH of around 8.7, which reveals that the isoelectric point (i.e.p.) of α-Al_2O_3 particles is 8.7 in sulfamate system.

The influence of metal ion concentration on zeta potentials of Al_2O_3 at pH = 3.0 is shown in Fig. 5. The zeta potential of α-Al_2O_3 increases with metal ion concentration. Furthermore, the zeta potential obtained from solutions containing Co^{2+} is more positive than that from solutions containing Ni^{2+} at the same metal ion concentration, which means that Co^{2+} adsorb more readily on the Al_2O_3 particle

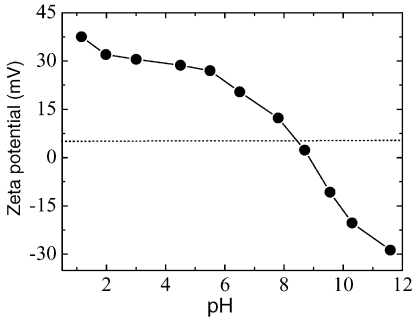

Fig. 4. Zeta potential of α-Al_2O_3 particles in 0.001 M NaCl supporting electrolyte at different pH.

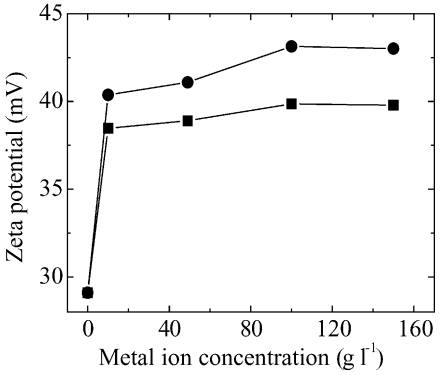

Fig. 5. Zeta potential of α-Al_2O_3 particles obtained from diluted electrolytes containing Ni^{2+}(■) and Co^{2+}(●) at pH 4.0.

surfaces than Ni^{2+} does. The results of zeta potential can well explain the experimental results in Fig. 3.

In order to investigate the competitive adsorption between Co^{2+} and Ni^{2+} on particle surface in solution, the zeta potentials in different Co^{2+}/Ni^{2+} ratio solutions were measured and shown in Fig. 6. More positive zeta potentials can be obtained with increase in Co^{2+} concentration when kept same total metal ion concentration. As shown in Figs. 5 and 3, compared with Ni^{2+}, Co^{2+} contributes more to the codeposition of Al_2O_3 particles due to its stronger adsorption on particle surface, which increases the surface positive charge.

Faradaic efficiency is the fraction of current utilized for metal deposition; part of current is usually taken up by the hydrogen evolution reaction. The effect of Al_2O_3 particles ($80\,g\,l^{-1}$) on current efficiencies during Co–Ni alloy codeposition in different Co^{2+}/Ni^{2+} ratio electrolytes (same total metal ion concentration) are also shown in Fig. 6. The results show that increasing Co^{2+} or decreasing Ni^{2+} concentration would contribute to improve current efficiency in codeposition.

3.3. Steady-state polarization curves

The effect of Al_2O_3 particles on the cathodic polarization behaviour was investigated in different Co^{2+}/Ni^{2+} ratio electrolytes (1:5 and 5:1). Fig. 7 shows the cathodic polarization curves for codeposition of Al_2O_3 with Co–Ni alloy in nickel-rich electrolytes ($Co^{2+}/Ni^{2+} = 1{:}5$) containing variable Al_2O_3 particle concentrations. The curves represent two consecutive reduction reactions, in which H^+ and Co^{2+}/Ni^{2+} are reduced to H_2 and Co–Ni alloy, respectively. Fig. 7 also indicates that Al_2O_3 particles lead to a potential shift to more negative direction with a gradual increase of Al_2O_3 particles, but the slopes are unchanged. These results reveal that the adsorption of particles on the cathode surface hinders the deposition of Ni^{2+}, but does not significantly affect the electrochemical reaction mechanism. From zeta potential, the adsorption of Ni^{2+} on particle surface is weak in nickel-rich Co–Ni alloy electrolytes, so the shift in reduction potential to negative assumedly is attributable to a shielded effect caused by adsorbed Al_2O_3 particles on electrode/electrolyte interfaces, which consequently, increases the activation polarization. From the microstructure of Co–Ni–Al_2O_3 composite coatings we have investigated previously [41], comparing to the Co–Ni alloy coating (Co content 20% wt.), a smaller Co–Ni alloy grain size is observed in the composite coating (Co content 16% wt.). A reasonable explanation is that the adsorption of Al_2O_3 on the cathode surface could increase cathodic polarization and contributes to develop fine grains. The similar results were also found by Socha et al. [29] in codeposition of SiC with Ni. The SiC particles block part of the electrode surface causing a current decrease. In consequence, the system is forced to produce new growth centres that result in a smaller Ni crystal size. According to above explanation, it seems reasonable that the effect increases with particle concentration due to the increasing amount of blocked sites on cathode surface.

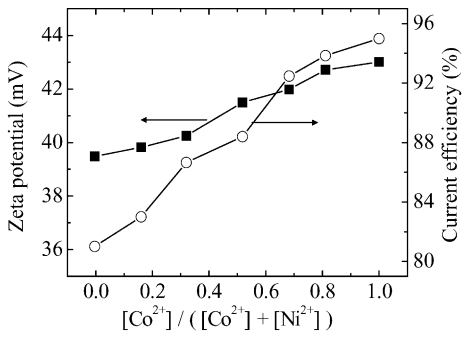

Fig. 6. Zeta potential (■) obtained from the diluted electrolytes containing different ratios of Co^{2+}/Ni^{2+} and current efficiency (○) of codeposition in these electrolytes.

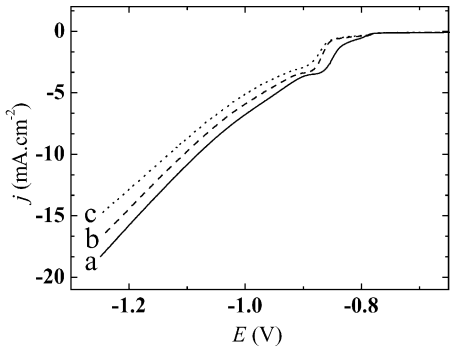

Fig. 7. Cathodic polarization curves for codeposition of Al_2O_3/Co–Ni alloys from nickel-rich electrolytes ($Co^{2+}/Ni^{2+} = 1{:}5$) with different concentrations of Al_2O_3 particles: (a) $0\,g\,l^{-1}$, (b) $40\,g\,l^{-1}$, (c) $80\,g\,l^{-1}$.

Comparing with Fig. 7, the effect of Al_2O_3 particles on polarization in cobalt-rich electrolytes ($Co^{2+}/Ni^{2+} = 5{:}1$) is quite contrary and shown in Fig. 8. Al_2O_3 particles lead to a positive shift in reduction potential and an increase in the cathodic current, but do not greatly affect the shape of the reduction wave. The positive shift (depolarization) is 140 mV at a concentration of $80\,g\,l^{-1}$ Al_2O_3. These deporlarization trends caused by inert particles were also observed by Watson and Walters [30,42] in their studies on the addition of SiC

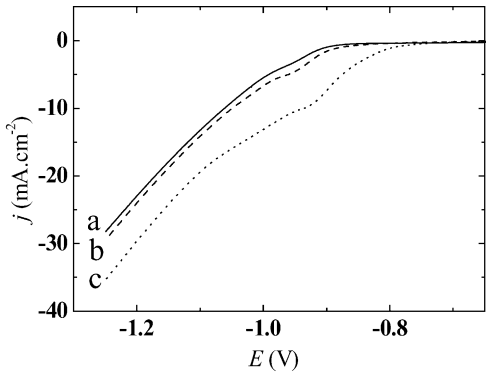

Fig. 8. Cathodic polarization curves for codeposition of Al_2O_3/Co–Ni alloys from cobalt-rich electrolytes (Co^{2+}/Ni^{2+} = 5:1) with different concentrations of Al_2O_3 particles: (a) 0 g l^{-1}, (b) 40 g l^{-1}, (c) 80 g l^{-1}.

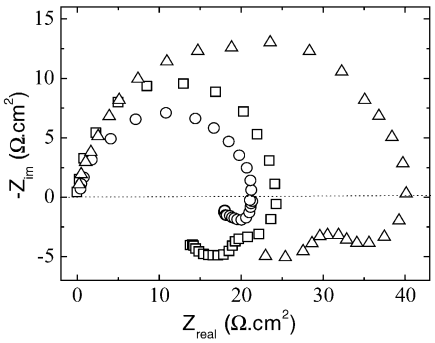

Fig. 9. Impedance spectra for codeposition of Al_2O_3/Co–Ni alloys from nickel-rich electrolytes (Co^{2+}/Ni^{2+} = 1:5) with different concentrations of Al_2O_3 particles: (○) 0 g l^{-1}, (□) 40 g l^{-1}, (△) 80 g l^{-1}.

and Cr particles to nickel sulfate electrolyte. Furthermore, in reference [41], comparing surface microstructure of Co–Ni alloy coating (Co content 78% wt.), the Co–Ni–Al_2O_3 composite coating (almost same Co content 80% wt.) exhibits relatively more larger grain size. The results reveal that in cobalt-rich electrolytes, the influence of depolarization of Al_2O_3 particles leads to bigger grain. A reasonable explanation maybe is due to the large amounts of Co^{2+} adsorption on particle surfaces, and then the diffusion of Co^{2+} near the cathode can be enhanced by the electrophoresis of Al_2O_3 particles. Gomez et al. [38] revealed the codeposition of Co–Ni alloys proceeds with simultaneous discharge of Co^{2+} under diffusion control and Ni^{2+} discharges under activation control. For this reason, a promotion of Co^{2+} diffusion is one of factors to enhance Co^{2+} reduction rate due to presence of particles. The results obtained from polarization curves are in good agreement with Fig. 1, in which Al_2O_3 increases the Co content in composite coatings.

3.4. Electrochemical impedance spectroscopy (EIS)

EIS measurements allow the elementary steps of an electrochemical reaction to be separated on the basis of different relaxation time constants. Therefore, the effects of Al_2O_3 particles on the codeposition of Co–Ni alloys were studied by EIS. The EIS experiments were performed at constant potential of −0.9 V, pH 4.0, 100 rpm, and 25 °C. Figs. 9 and 10 recorded EIS results (Nyquist plots) of codeposition with various Al_2O_3 concentrations into the nickel-rich (Co^{2+}/Ni^{2+} = 1:5) and cobalt-rich (Co^{2+}/Ni^{2+} = 5:1) electrolytes, respectively. The *jR* drop has been corrected. From Figs. 9 and 10, when the Al_2O_3 particles were added, besides one capacitive loop at high frequency and one inductive loop at low frequency, another one inductive loop is presented at low frequency. The capacitive loop at very high frequency can be interpreted as the electrical double layer capacitance C_{dl} in parallel with a charge transfer resistance R_{ct}, and the first inductive loop maybe is the result of the relaxation or lessening of the cathodes covered by an intermediate species, which affects the deposition of Co–Ni alloys [4]. The second inductive loop at very low frequency maybe is due to the adsorption and desorption of Al_2O_3 particles on cathode surface. The impedance studies suggest that electrodeposition of Co–Ni alloys with or without Al_2O_3 particles is a multi-step reaction process involving surface adsorbed intermediates produced by the charge transfer reaction and the removal of the adsorbed intermediates by a subsequent consumption reaction.

Fig. 11 shows the equivalent circuit representing the electrochemical behaviour of composite codeposition of Al_2O_3 particles with Co–Ni alloys. According to the Armstrong equivalent electric circuit, the Faradaic impedance, Z_F is defined as follow [43,44]:

$$Z_F = \left[\frac{1}{R_{ct}} + \frac{R_{01} + R_{02} + j\omega(L_1 + L_2)}{R_{01}R_{02} - \omega^2 L_1 L_2 + j\omega(R_{01}L_2 + R_{02}L_1)}\right]^{-1}$$

In this circuit, R_{el} represents the solution resistance, R_{ct} the charge transfer resistance, C_{dl} the double layer capacitance, L_1 the inductance and R_{01} the resistance from the adsorbed intermediates and L_2 the inductance and R_{02} the resistance from the adsorbed Al_2O_3 particles on the electrode surface. In general, higher rate reactions appear at higher frequency range on the impedance spectra, while adsorbed films and inhibitory effect appear at lower frequency range. L and R_0

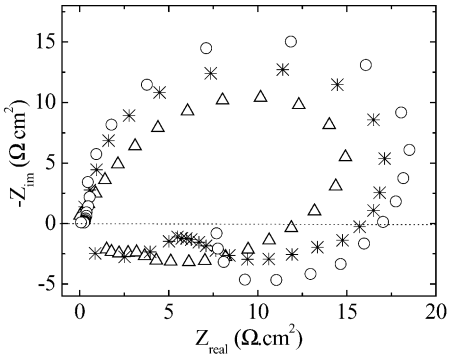

Fig. 10. Impedance spectra for codeposition of Al_2O_3/Co–Ni alloys from cobalt-rich electrolytes (Co^{2+}/Ni^{2+} = 5:1) with different concentrations of Al_2O_3 particles: (○) 0 g l^{-1}, (*) 40 g l^{-1}, (△) 80 g l^{-1}.

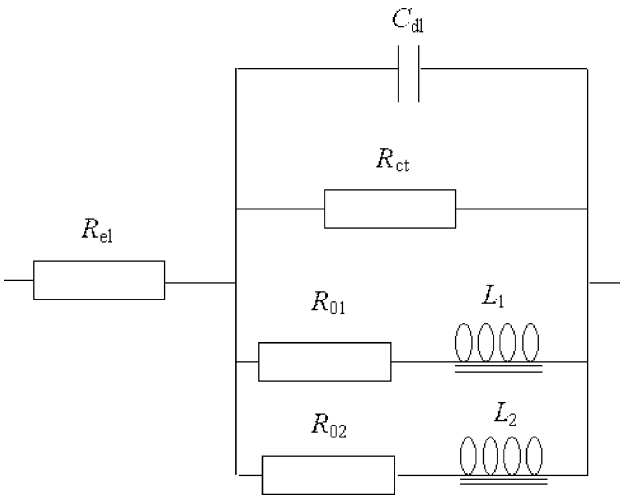

Fig. 11. Equivalent circuit used for simulating the impedance spectra for codeposition of Al_2O_3 with Co–Ni alloys.

are often used to account for the inductive loop at low frequency, which is caused by adsorbed/desorbed intermediates or other species on the electrode surface. The magnitude of the R_{ct} is an indicator of the easiness of the electrochemical reaction.

According to the equivalent circuit, the simulated values of the impedance parameters for the codeposition were determined by CNLLS fitting procedure and listed in Table 2. It can be found that the effect of Al_2O_3 particles on the Co–Ni codeposition in different electrolytes is quite different. In nickel-rich electrolytes ($Co^{2+}/Ni^{2+} = 1{:}5$), the R_{ct} becomes larger with increasing Al_2O_3 concentration. So it can be confirmed that the Al_2O_3 particles adsorbed on the cathode shield active sites for reduction of Ni^{2+} ions on cathode surface. But the opposite results were obtained in cobalt-rich electrolytes ($Co^{2+}/Ni^{2+} = 5{:}1$). The addition of Al_2O_3 particles leads to a decrease of R_{ct} and means to active the reduction of Co^{2+}. Due to the results of Figs. 5 and 6, Al_2O_3 particles have stronger tendency to adsorb Co^{2+} than Ni^{2+}. The activation of particles to reduction of Co^{2+} maybe relate to not only an enhancement of Co^{2+} diffusion but an interaction between Co^{2+} and Al_2O_3 surfaces. In Table 2, the values of L_1 obtained from cobalt-rich electrolytes are larger than that from nickel-rich electrolytes. The results reveal that the probably increasing intermediate on the electrode surface is $Al_2O_3Co^{+}_{ads}$, which is easier to produce and result in a larger inductance value due to the stronger adsorption of Co^{2+} on particle surfaces.

From Fig. 1, the curves of V_p versus Al_2O_3 concentration are very similar to the well-known Langmuir adsorption isotherm supporting a mechanism based on an adsorption effect. So L_2 may be attributed to the adsorption of Al_2O_3 particles on the cathode surface and increases with Al_2O_3 concentrations. Furthermore, it can be noted that L_2 from cobalt-rich electrolytes is also larger than that from nickel-rich electrolytes. A reasonable explanation is that the adsorption of Co^{2+} increases the particle surface positive charge density and probably strengthens the adsorption strength between particles and cathode surfaces. The results are coincident with Fig. 2, which Co^{2+} promotes the codeposition of Al_2O_3 particles.

4. Discussion

The effect of Al_2O_3 particles on polarization behaviours and impedance parameters of Co–Ni alloy codeposition had investigated in above experiments. It can be confirmed that in nickel-rich electrolytes, the Al_2O_3 particles cause an obstructive effect on the Ni^{2+} deposition due to the adsorption of Al_2O_3 particles on the cathode surface. The metal ions in electrolytes can be classified two kinds: one is freely solvated metal ion and the other is adsorbed metal ion on particle surface. In the literatures [25,26], it has been demonstrated that metal ions and hydrogen ions absorbed on particle surfaces can be reduced. However comparing Co^{2+}, the adsorption of Ni^{2+} on Al_2O_3 particle surface is weak, and the freely solvated Ni^{2+} is majority in nickel-rich electrolytes. So a mainly reasonable explanation to inhibition of Ni^{2+} reduction is shielded effect of Al_2O_3 particles adsorbed on cathode surface, even if other factors such as the modification of reaction activation energy and adsorption isotherms of Ni^{2+} still occur. In cobalt-rich electrolytes, due to strong adsorption of Co^{2+} on the Al_2O_3 particle surfaces, the reduction of Co^{2+} is activated by an enhancement of Co^{2+} diffusion and an interaction between Co^{2+} and Al_2O_3.

According to the present state of knowledge about electrocrystallization of polyvalent metal, it is accepted in recent years that the electrodeposition of Me^{2+} (Me = metal) occurs in several steps. More particularly, most authors

Table 2
Simulated parameters of the equivalent circuit for codeposition of Al_2O_3 with Co–Ni alloys

Electrolytes, Co^{2+}/Ni^{2+}	Al_2O_3 ($g\,l^{-1}$)	R_{ct} ($\Omega\,cm^2$)	C_{dl} ($\mu F\,cm^{-2}$)	L_1 ($H\,cm^2$)	R_{01} ($\Omega\,cm^2$)	L_2 ($H\,cm^2$)	R_{02} ($\Omega\,cm^2$)
1:5	0	21.5	100.3	2.8	4.8	–	–
	40	24.8	78.5	3.7	8.1	0.32	13.6
	80	41.2	69.1	4.3	11.7	0.48	16.2
	0	18.5	90.2	5.8	10.1	–	–
5:1	40	16.8	61.0	8.7	13.2	0.41	7.8
	80	15.2	43.2	9.8	16.7	0.56	18.5

agreed that an intermediate Me^+ adsorbed on the electrode is formed during the cathodic reaction of the electrodeposition of nickel and cobalt in acidic medium. However, the more details about electrochemical reactions leading to metal are still a matter for discussion, and the intermediate, Me^+_{ads} is considered to be either a catalyst or a compound, which is consumed at the electrode.

During Co–Ni alloy electrodeposition, the localized concentration of hydroxide ions near the cathode surface will increase and result in the intermediate formation, $MeOH_{ads}$ ($NiOH_{ads}$ and $CoOH_{ads}$).

The discharge arises from the ion $(MeOH)^+$ formed by the following chemical reaction.

$$Me^{2+} + H_2O \rightarrow (MeOH)^+ + H^+ \quad (1)$$

This ion adsorption occurs according to the electrochemical reaction (2).

$$(MeOH)^+ + e^- \rightarrow Me(OH)_{ads} \quad (2)$$

As for deposition of Ni^{2+}, the mechanism is described as below.

$$Ni(OH)_{ads} + e^- \rightarrow Ni + OH^- \quad (3)$$

$$Ni(OH)_{ads} + (NiOH)^+ + 2e^- \rightarrow Ni + OH^- + Ni(OH)_{ads} \quad (4)$$

This mechanism was first proposed by Epelboin et al. [45] with more discussion by Chassaing et al. [46]. Reactions (3) and (4) are the most likely paths for nickel reduction with no particles in acidic electrolyte.

As a result of weak adsorption of Ni^{2+} on Al_2O_3 particle surfaces in nickel-rich electrolytes, the freely solvated Ni^{2+} is predominant, so the effect of Al_2O_3 on the reduction of Ni^{2+} is just considered to block some of active sites at the cathode/electrolyte interfaces. Consequently, the adsorption of particles on cathode causes an increase of cathodic polarization. Furthermore, taking into account the experimental results of current efficiency, comparing to Ni^{2+}, the adsorption of H^+ on Al_2O_3 particle surfaces is larger so Al_2O_3 particles in nickel-rich electrolytes maybe preferentially catalyze H_{ads} intermediate. The proof that H_{ads} intermediate is catalyzed by inert particles in electrolyte was revealed by current efficiency studies, hydrogen analysis and X-ray diffraction analysis of composite electrodeposited coatings [31]. So the following reactions are possible.

$$Al_2O_3 \cdot H^+ + e^- \rightarrow Al_2O_3 \cdot H_{ads},$$

$$Al_2O_3 \cdot H_{ads} + H^+ + e^- \rightarrow Al_2O_3 + H_2 \uparrow$$

In cobalt-rich electrolytes, from the polarization curves, the addition of Al_2O_3 particles does not affect the shape of reduction wave and only shift the wave to a more positive potential. This means that Al_2O_3 particles do not significantly affect the electrochemical reaction mechanism. Near the cathode surface, comparing freely solvated Co^{2+}, the adsorbed Co^{2+} on Al_2O_3 particle surface assumes significant. So the reduction mechanism of adsorbed Co^{2+} might be as follow:

$$Al_2O_3 + Co^{2+} + H_2O \rightarrow Al_2O_3(CoOH)^+ + H^+ \quad (5)$$

$$Al_2O_3 \cdot (CoOH)^+ + e^- \rightarrow Al_2O_3 \cdot Co(OH)_{ads} \quad (6)$$

$$Al_2O_3 \cdot Co(OH)_{ads} + e^- \rightarrow Al_2O_3 + Co + OH^- \quad (7)$$

$$Al_2O_3 \cdot Co(OH)_{ads} + (CoOH)^+ + 2e^- \rightarrow Al_2O_3 + Co + OH^- + Co(OH)_{ads} \quad (8)$$

$$Co(OH)_{ads} + e^- \rightarrow Co + OH^- \quad (9)$$

According to Heusler and Galser [47], like $Me(OH)_{ads}$, the $Al_2O_3{\cdot}Co(OH)_{ads}$ can be considered to be not only an intermediate but also a catalyst. So in cobalt-rich electrolytes, the Al_2O_3 particles carrying a large amount of Co^{2+} contribute to produce intermediate $Al_2O_3{\cdot}Co(OH)_{ads}$, which have catalytic activity to subsequent reaction (7) and (8) on the electrode surface. Furthermore, in cobalt-rich electrolytes the difference of L_1 between with and without Al_2O_3 particles is larger than that in nickel-rich electrolytes. This means that with addition of Al_2O_3 particles, the probably intermediates $Al_2O_3{\cdot}Co(OH)_{ads}$ is incremental, so the total adsorptions of $Al_2O_3{\cdot}Co(OH)_{ads}$ and $Co(OH)_{ads}$ on the electrode surface would result in a larger L_1 value. Consequently, the first inductive loop shown in Nyquist plots of Co–Ni codeposition with and without particles is attributed to adsorbed intermediate, $Me(OH)_{ads}$ and $Al_2O_3{\cdot}Co(OH)_{ads}$, being produced on the electrode.

Moreover, in cobalt-rich electrolytes, the effect of Al_2O_3 particles on H^+ reduction is not prominent. Yeh and Wan [4] noticed that when the pH in electrolytes is below the isoelectric point (i.e.p.), the effect of particles on current efficiency in composite electrodeposition would be remarkably. So according to the result of Yeh and Wan, the tendency to H^+ adsorption on the Al_2O_3 particle surfaces and the decrease in current efficiency would be dominant in composite codeposition electrolytes with a pH of 4.0 which lower than isoelectric point (i.e.p.) of Al_2O_3 in sulfamate electrolytes 8.7. However, in cobalt-rich electrolytes, due to strong interaction between Al_2O_3 particles and Co^{2+}, so the effect of particles on H^+ reduction is weak enough to ignore.

5. Conclusions

The effect of Al_2O_3 particles on electrochemical behaviours of Co–Ni alloy codeposition was investigated in this paper. The measurements of zeta potential indicate that in sulfamate system the isoelectric point (i.e.p.) of α-Al_2O_3 particles is 8.7 and the adsorption of Co^{2+} on particle surface is much stronger than Ni^{2+}. Due to the strong interaction between the Al_2O_3 particles and Co^{2+}, their deposition can promote each other during composite

codeposition in sulfamate electrolytes. By electrochemical investigations including polarization curves and EIS, the effect of Al_2O_3 on codeposition of Co–Ni alloy in nickel- and cobalt-rich electrolytes is quite different. In nickel-rich electrolytes ($Co^{2+}/Ni^{2+} = 1:5$), the Al_2O_3 particles cause a shift in negative direction for reduction potential and an increase of charge transfer resistance. The reduction of Ni^{2+} is inhibited due to the obstruction of Al_2O_3 particles on cathode surface. However, in cobalt-rich electrolytes ($Co^{2+}/Ni^{2+} = 5:1$), Al_2O_3 particles lead to a positive shift of reduction potential and reduce the charge transfer resistance. The reduction of Co^{2+} is activated. The enhancement of Co^{2+}diffusion near the cathode and production of intermediate $Al_2O_3{\cdot}Co(OH)_{ads}$ on cathode surface all promote Co^{2+} reduction reaction during composite electrodeposition. In addition, taking into account the results of current efficiency, in nickel-rich electrolytes, the Al_2O_3 particles may catalyze H_{ads} and enhance hydrogen evolution reaction, while the effect of Al_2O_3 particles on hydrogen reduction is insignificant in cobalt-rich electrolytes.

According to simulation of impedance spectra for codeposition of Al_2O_3 with Co–Ni alloys, the first inductive loop of Nyquist plots in low frequency region with and without particles is attributed to adsorbed intermediate, $Me(OH)_{ads}$ and $Al_2O_3{\cdot}Co(OH)_{ads}$, being produced on the electrode. The second inductive loop appeared in low frequency region probably is caused by adsorption and desorption process of Al_2O_3 particles on the electrode surface.

Acknowledgements

The authors thank Shanghai BaoShan Iron and Steel Company and High-New Technique Development Project of ShanDong province China for financial support.

References

[1] A. Hovestad, L.J.J. Janssen, J. Appl. Electrochem. 25 (1995) 519.
[2] M. Musiani, Electrochim. Acta 45 (2000) 3397.
[3] C. Kerr, D. Barker, F. Walsh, Trans. Inst. Met. Finish. 78 (2000) 171.
[4] S.H. Yen, C.C. Wan, J. Appl. Electrochem. 24 (1994) 993.
[5] B. Szcygiel, Trans. Inst. Met. Finish. 75 (1997) 59.
[6] K.K. Sun, J.Y. Hong, Surf. Coat. Technol. 108 (1998) 564.
[7] P. Nowak, R.P. Socha, M. Kaisheva, J. Fransaer, J.P. Celis, Z. Stoinov, J. Appl. Electrochem. 30 (2000) 429.
[8] M.H. Fawzy, M.M. Ashour, A.M.A. Halim, Trans. Inst. Met. Finish. 74 (1996) 72.
[9] J. Li, C.S. Dai, D.L. Wang, X.G. Hu, Surf. Coat. Technol. 91 (1997) 131.
[10] E.P. Rajiv, S.K. Seshadri, Plat. Surf. Finish. 80 (1993) 66.
[11] D. Aslanidis, J. Fransaer, J.P. Celis, J. Electrochem. Soc. 144 (1997) 2352.
[12] N.A. Assuncao, M.D. Giz, G. Tremiliosi, E. Gonzalez, J. Electrochem. Soc. 144 (1997) 2794.
[13] L.B. Albertini, A.C.D. Angelo, E. Gonzalez, J. Appl. Electrochem. 22 (1992) 888.
[14] A.C. Tavares, S. Trasatti, Electrochim. Acta 45 (2000) 4195.
[15] R. Bocutti, M.J. Saeki, A.O. Florention, C.L.F. Oliveira, A.C.D. Angelo, J. Int. Hydrogen Energy 25 (2000) 1051.
[16] G. Wu, N. Li, C.S. Dai, D.R. Zhou, Mater. Chem. Phys. 83 (2004) 307.
[17] B. Szcaygiel, Plat. Surf. Finish. 84 (1997) 62.
[18] J.L. Guichard, A. Mocellin, M.O. Simonnot, J.F. Remy, M. Sardin, Powder Technol. 99 (1998) 257.
[19] C.G. Fink, J.D. Prince, J. Electrochem. Soc. 54 (1928) 315.
[20] T.W. Tomaszewski, L.C. Tomaszewski, H. Brown, Plating 56 (1969) 1234.
[21] A.M.J. Kariapper, J. Foster, Trans. Inst. Met. Finish. 52 (1974) 87.
[22] K. Meguno, T. Ushida, T. Hiraoka, K. Esumt, Bull. Chem. Soc. Jpn. 60 (1987) 89.
[23] C.C. Lee, C.C. Wan, J. Electrochem. Soc. 135 (1988) 195.
[24] N. Guglielmi, J. Electrochem. Soc. 119 (1972) 1009.
[25] J.P. Celis, J.R. Roos, C. Buelens, J. Electrochem. Soc. 134 (1987) 1402.
[26] J. Fransaer, J.P. Celis, J.R. Roos, J. Electrochem. Soc. 139 (1992) 413.
[27] D.L. Wang, J. Li, C.S. Dai, X.G. Hu, J. Appl. Electrochem. 29 (1999) 437.
[28] M. Holm, T.J. O'Keefe, J. Appl. Electrochem. 30 (2000) 1125.
[29] R.P. Socha, P. Nowak, K. Laajalehto, J. Vayrynen, Colloids Surf. A: Physicochem. Eng. Aspects 235 (2004) 45.
[30] S.W. Watson, J. Electrochem. Soc. 140 (1993) 2235.
[31] L. Benea, G. Carac, Cercet. Met. Noi. Mater. 5 (1997) 20.
[32] D. Golodnitsky, N.V. Gudin, G.A. Volyanuk, Plat. Surf. Finish. 85 (1998) 65.
[33] A.N. Correia, S.A.S. Machado, Electrochim. Acta 45 (2000) 1733.
[34] H.B. Suffredini, J.L. Cerne, F.C. Crnkovic, S.A.A. Machado, J. Int. Hydrogen Energy 25 (2000) 415.
[35] S. Armyanov, Electrochim. Acta 45 (2000) 3323.
[36] L. Burzynska, E. Rudnik, Hydrometallurgy 54 (2000) 133.
[37] I. Epelboin, R. Wiart, J. Electrochem. Soc. 118 (1971) 1577.
[38] E. Gomez, J. Ramirez, E. Valles, J. Appl. Electrochem. 28 (1998) 71.
[39] S. Goldbach, R.D. Kermadec, F. Lapicque, J. Appl. Electrochem. 30 (2000) 277.
[40] Y. Zhuang, E.J. Podlaha, J. Electrochem. Soc. 147 (2000) 2231.
[41] G. Wu, N. Li, D.R. Zhou, K. Mitsuo, J. Mater. Sci. Technol. 19 (1) (2003) 133.
[42] S.W. Watson, R.P. Walters, J. Electrochem. Soc. 138 (1991) 3633.
[43] C.N. Cao, Electrochim. Acta 35 (1990) 837.
[44] J.R. Macdonald, J. Schoonman, A.P. Leher, J. Electroanal. Chem. 131 (1982) 77.
[45] I. Epelboin, M. Joussellin, R. Wiart, J. Electroanal. Chem. 61 (1981) 119.
[46] E. Chassaing, M. Joussellin, R. Wiart, J. Electroanal. Chem. 75 (1983) 157.
[47] K.E. Heusler, L. Galser, Electrochim. Acta 13 (1968) 59.